Biochimica et Biophysica Acta, 433 (1976) 457–468

BBA 77296

PHASE TRANSITIONS OF PHOSPHOLIPID SINGLE-WALL VESICLES AND MULTILAYERS

MEASUREMENT BY VIBRATIONAL RAMAN SPECTROSCOPIC FREQUENCY DIFFERENCES

ROBERT C. SPIKER, Jr and IRA W. LEVIN

Laboratory of Chemical Physics, National Institute of Arthritis, Metabolism and Digestive Diseases, National Institutes of Health, Bethesda, Md. 20014 (U.S.A.)

(Received October 20th, 1975)

SUMMARY

Raman spectroscopic frequency differences between selected carbon-carbon stretching modes of lipid hydrocarbon chains were determined as a function of temperature for use in monitoring lipid phase transition behavior and acyl chain disorder in both multilamellar and single-wall vesicles. Transition temperatures detected by this procedure for pure dipalmitoyl phosphatidylcholine and dimyristoyl phosphatidylcholine multilayers were observed at 39 ± 1 °C and 23 ± 1 °C, respectively. Although the phase transition for unilamellar vesicles of dipalmitoyl phosphatidylcholine occurred at nearly the same temperature as the multilayers, the crystal-liquid crystalline transition for the single-shell vesicles appeared to span a slightly broader temperature range, a characteristic consistent with irregularities in the packing arrangement of the hydrocarbon chains. Within the precision of the Raman spectroscopic method, however, the temperature behavior of both the multilamellar and the unilamellar dimyristoyl phosphatidylcholine assemblies appeared nearly identical. The temperature profile for the Raman frequency differences of an excess water sonicate of 25 mol percent cholesterol in dipalmitoyl phosphatidylcholine served as an example of the effect upon lipid phase transition characteristics of a bilayer component intercalated between the acyl chains. For this particular cholesterol-lipid system the phase transition was broadened over a 30 °C temperature range, in contrast to the narrow 2–4 °C range observed for pure multilayer and single-shell vesicle particles.

INTRODUCTION

The study of lipid phase transitions in both model and natural membrane systems has proved to be a productive approach toward understanding the structure, organization and interactions present in lipid bilayer assemblies (for example refs. 1–3). For example, the effects of temperature on lipid miscibility and the relation of crystal-

liquid crystalline phase transitions to lateral lipid phase separations in membranes have recently become active areas of inquiry [1, 4–6]. Although diverse physical methods are employed for specifically examining phase transition behavior, as well as a variety of other structural aspects of membrane components [1–3, 7], it remains of continuing interest to extend and to refine techniques which directly reflect relevant dynamic properties of the bilayer system.

Recently, the conformational properties of multilamellar lipid systems undergoing either environmental perturbations or phase transition effects were shown to be reflected by changes in intensity of certain vibrational transitions detected by Raman and infrared spectroscopic techniques [8–15]. Raman intensities originating from two types of vibrational distortions, the methylene stretching modes occurring in the 2850–2900 cm^{-1} spectral region and the carbon-carbon (C-C) stretching modes arising in the 1100 cm^{-1} area, were particularly useful in detecting structural changes within the lipid hydrocarbon skeleton. As a complement to relative intensity observations, the present study emphasizes the sensitivity of the frequency shifts of various C-C stretching vibrations to hydrocarbon rotamer formation arising from either temperature or intermolecular effects. Since Raman and infrared spectroscopic frequency and frequency difference measurements are directly related to the structural and bonding characteristics of a chemical system through, for example, detailed normal coordinate analyses, these frequency parameters provide an additional sensitive and selective molecular probe for investigating lipid bilayer behavior on the vibrational time scale. In the current study we demonstrate the use of precise vibrational frequency shift information to monitor the gel-liquid crystalline phase transition of lipid bilayers in both the multilamellar and single-wall vesicle forms of dipalmitoyl phosphatidylcholine/water and dimyristoyl phosphatidylcholine/water mixtures. The frequency shift parameters of a cholesterol/phosphatidylcholine/water system are also examined as a function of temperature in order to contrast the spectroscopic behavior of a melting process with diminished cooperativity to that of a pure lipid bilayer.

EXPERIMENTAL

High purity samples of 1,2 dipalmitoyl-D,L-phosphatidylcholine, cholesterol and L-α-dimyristoyl phosphatidylcholine were obtained commercially from Sigma Chemical Co., Supelco, Inc. and Nutritional Biochemicals Corp., respectively. These samples gave a single spot by thin-layer chromatography and produced no major spectral contaminants; therefore, they were used without further purification. Dipalmitoyl phosphatidylcholine/cholesterol mixtures were prepared by dissolving weighed amounts of the components in chloroform and drying first by a stream of nitrogen, then in vacuo. Vesicles (~ 250 Å) [16–17] of 30 % dipalmitoyl or dimyristoyl phosphatidylcholine by weight in water were prepared by sonicating to clarity for 20–40 min at temperatures above their respective gel-liquid crystalline transition points. A Branson probe type sonicator equipped with a microtip was used to prepare the single-wall vesicle systems. Vesicle preparations were verified by electron microscopy. No differences in spectra were observed for vesicles prepared at the extremes of this time span. Centrifugation was employed to remove any small amounts of either multilayers or larger vesicles from the samples. The dipalmitoyl phosphatidylcholine/cholesterol (25 mol %)/water suspension was made by sonicating the previously

prepared dry mixture in excess water in a bath type sonicator about 30 min at elevated temperatures. Dipalmitoyl and dimyristoyl phosphatidylcholine multilayers (30 % by weight in water) were prepared by vortex mixing for 10–20 min with occasional heating above their transition temperatures.

Raman spectra were obtained with a Cary Model 81 spectrophotometer equipped with a Coherent Radiation Model 52 argon ion laser source. The laser was typically operated to give 300–900 M_r of 5145 Å or 4880 Å radiation incident upon the sample. Spectral resolution varied between 2 and 5 cm^{-1}. Absolute spectral frequencies, calibrated with atomic argon lines, are determined to ± 2 cm^{-1}. The frequency difference parameters, however, are determined to 0.25–0.50 cm^{-1} with suitable scale expansions.

Sample spectra were recorded utilizing two different optical arrangements and a variety of sampling techniques. The dipalmitoyl phosphatidylcholine/cholesterol spectra were measured using the standard Cary 81 optical arrangement and a variable temperature vacuum cell, which has been previously described [18]. This cell was modified for high temperature work by placing several turns of nichrome wire around the support finger of the copper scatter plate. A copper-constantan thermocouple was soldered to the copper plate about 3 mm from the sampling area. Thermocouple voltages were monitored by a Kin Tel microvolt-ammeter and a Keithley 160 Digital Multimeter, both of which were calibrated by a Dynage, Inc. voltage calibrator (± 0.1 %). All other spectra were recorded with a new external optical system designed for use with the basic Cary monochromator and detection equipment [15]. The almost transparent vesicle solutions were placed in a standard 1 cm^2 cuvette, which was wrapped with nichrome wire for heating. The thermocouple was immersed in the solutions near the laser beam transit. Spectral quality was enhanced by multipassing the laser beam through the cell. Multilayer samples were placed in a 1 cm tube and again the thermocouple was placed close to the point of laser beam contact. The melting point of dipalmitoyl glycerine (63 °C) was used to check the accuracy of the thermocouple arrangement and was found to be good to ± 1 °C. For attaining temperatures below ambient, a stream of cooled nitrogen gas was directed at the sample containers. Temperature change (± 1 °C) was achieved simply by altering the flow rate. Sample heating by the laser beam (3 °C or less) was minimized by using the larger cells instead of capillary tubes. Equilibration of the lipid systems at each temperature was verified by multiple spectroscopic scans over a several hour period. Temperature behavior was reversible as demonstrated by passing back through the phase transition to repeat spectroscopic scans for previous temperatures.

RESULTS AND DISCUSSION

A. Frequency difference measurements involving C-C stretching vibrations

The characteristic C-C skeletal frequency shifts which we will specifically monitor occur within the 1065, 1100 and 1130 cm^{-1} spectral regions. On increasing the temperature of a lipid bilayer system below the crystal-liquid crystalline transition temperature, the Raman spectral transitions, which are assigned at low temperatures to the all-*trans* hydrocarbon C-C stretching modes, exhibit moderate frequency shifts (and intensity changes) as *gauche* structures are gradually introduced into the acyl chains. As the system passes through the phase transition, larger frequency shifts

occur during the cooperative melting process of the chains. Finally, during temperature changes above the phase transition point the skeletal modes again display gradual frequency shifts while further *gauche* conformations are formed and populated.

We may compare the frequency shift behavior with the concomitant changes in Raman intensities [8–14]. Thus, below the transition temperature of the bilayer, the Raman intensity of the 1100 cm^{-1} feature increases, while the intensities of the 1130 and 1065 cm^{-1} transitions decrease. These intensity alterations parallel the increasing number of *gauche* conformations. The most dramatic intensity change occurs above the transition temperature, at which point the central 1100 cm^{-1} feature predominates. Thus, as individual transitions for the new *gauche* bonds appear and increase the intensity of the 1100 cm^{-1} feature, the peak frequency, or center of gravity, of this broadened central band shifts to lower wavenumbers. The appearance of these new C-C stretching modes within the 1100–1065 cm^{-1} region is confirmed by normal coordinate calculations performed on various *n*-paraffin systems [19].

The observed frequencies and frequency shifts reflect the inherent changes in the vibrational kinetic and potential energy energies of the system [20] as the C-C bond angles rotate to accommodate the formation of rotational isomers. Since the intramolecular potential energy terms of an acyl chain are not appreciably affected by the occurrence of rotational isomers [19], we may better understand the origin of the frequency shifts by examining the dependence of the vibrational kinetic energy upon the angle of C-C bond rotation τ. (See ref. 20, for example, for the methodology involved in relating the molecular structure parameters to the vibrational kinetic energy.) Thus, when the vibrational kinetic energy of the hydrocarbon chain is expressed in terms of the momenta conjugate to the various C-C stretching and C-C-C angle bending displacement coordinates, the functional dependence of the angle of internal rotation τ is introduced indirectly to the stretching frequencies through a coupling of the momenta terms for both the C-C stretching and C-C-C angle bending distortions. In contrast, the skeletal bending frequencies depend directly upon the rotational angle since terms for the bending modes alone include τ. Unfortunately, the weak Raman intensities of the chain bending modes, as compared to the stretching vibrations, preclude their use in following structural changes in lipid bilayers with our present instrumentation.

In experimentally monitoring the effects of the lipid phase transition upon the vibrational modes in the 1100 cm^{-1} region, it is convenient to present the temperature profile data in terms of a frequency difference parameter Δ, where, for example, $\Delta(1095\text{–}1065)$ cm^{-1} represents the frequency difference for a specified temperature between the spectral transitions occurring near 1095 cm^{-1} and 1065 cm^{-1}, respectively. We emphasize the measurement of a Δ cm^{-1} value for two reasons. First, Δ cm^{-1} can be measured accurately and reproducibly from a spectral trace. It is independent of laser and instrumental characteristics which may critically affect Raman intensity measurements. Since direct values for frequency differences are independent of a wavelength calibration, frequency differences obtained during separate experiments are easily compared. Second, experimental Δ cm^{-1} values are easily related to normal coordinate calculations performed on model paraffin systems; and frequency differences between various vibrational modes, rather than the absolute frequency values, become the relevant parameters for assessing the importance of specific

gauche conformations. For example, in using an intramolecular potential function developed specifically for hydrocarbon systems [19] to describe the lipid acyl chains, a close correspondence between the calculated and observed bilayer frequencies is not necessarily expected. The frequency differences Δ cm^{-1}, however, then become the meaningful constraint for extracting structural information from the observed spectrum. Calculations following this approach will be presented at a later date.

B. Temperature profiles for single-shell vesicle and multilayer assemblies of dipalmitoyl and dimyristoyl phosphatidylcholine

In order to determine the lipid phase transition, a frequency difference Δ cm^{-1}, corresponding to a pair of C-C stretching mode transitions from the 1065, 1100 or 1130 cm^{-1} region, is plotted as a function of temperature with the midpoint of the steep portion of the sigmoidal curve taken as the gel-liquid crystalline transition temperature. For the relatively sharp and symmetrical 1064 and 1129 cm^{-1} transitions, differences are determined to $\pm$0.25 cm^{-1} for a suitable scale expansion of the spectral trace. For measurements involving the broader and more asymmetrical 1097 and 1090 cm^{-1} features, which appear in dipalmitoyl and dimyristoyl phosphatidylcholine, respectively, differences are determined to $\pm$0.50 cm^{-1}. Although the weak phosphate PO_2^- symmetric stretching mode occurs about 1080 cm^{-1} [15], we assume that this transition does not appreciably perturb the frequencies of the $\sim$1100 cm^{-1} C-C stretching modes arising from the *gauche* structures. In addition, we assume that the intensity of the phosphate feature does not significantly increase as the bilayer temperature, particularly above the transition point, is raised. In general, the evidence from simpler model systems supports these assumptions.

Only two of the possible three Δ cm^{-1} parameters were used in determining transition temperatures. These involved either the 1064 and 1129 cm^{-1} transitions or the 1097 (or 1090) and 1064 cm^{-1} transitions. Over the temperature ranges studied, the 1064 cm^{-1} band shifted less than 2 cm^{-1} to about 1066 cm^{-1} for all systems, while the 1129 cm^{-1} feature shifted to about 1125 cm^{-1} at the higher temperatures*. The 1097 cm^{-1} band in dipalmitoyl phosphatidylcholine and the 1090 cm^{-1} band in dimyristoyl phosphatidylcholine shifted to about 1088 and 1086 cm^{-1}, respectively. Thus, the 1097 (or 1090) and 1129 cm^{-1} pairing was not used since the shift of both features in the same direction with increasing temperature provides a smaller and less certain frequency shift range for study. While the 1129 and 1064 cm^{-1} transitions retained fairly narrow half-widths and were symmetrical over most of the temperature range, the 1097 or 1090 cm^{-1} features were more asymmetrical and consequently provided slightly less accurate difference measurements. By following, however, the center of gravity movement of these transitions with temperature, satisfactory results are obtained. Therefore, we suggest that a plot of Δ(1129–1064) cm^{-1} against tem-

* Normal coordinate calculations suggest a basis for the larger shift of the 1129 cm^{-1} transition relative to the 1064 cm^{-1} transition [19]. The potential energy distributions calculated, for example, for *trans-trans-trans*, *trans-gauche-trans* and *gauche-trans-trans* *n*-C_6H_{14} rotational isomers [19] indicate that the higher frequency C-C stretching mode (which in the lipid system occurs about 1129 cm^{-1} as compared to 1140 cm^{-1} in the *n*-C_6H_{14} systems) is the only skeletal stretching vibration coupled to a C-C-C angle bending mode. Since the C-C-C angle bending frequencies are direct functions of the internal rotation angles, vibrations strongly coupled to these modes will more clearly reflect conformational rearrangements.

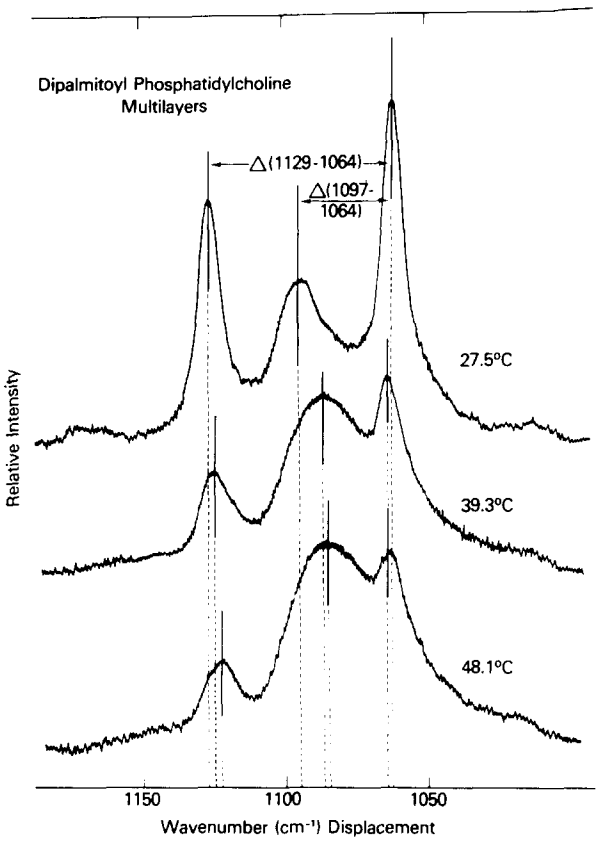

Fig. 1. Method used for determining frequency differences in dipalmitoyl phosphatidylcholine multilayers at various temperatures. Shown are Δ(1129–1064) and Δ(1097–1064) cm^{-1} measurements at 27.5, 39.3 and 48.1 °C which span the gel-liquid crystal transition.

perature provides the most accurate determination of transition temperatures by this method, although results using the Δ(1097–1064) cm^{-1} combination provide, within 1 °C, the same transition temperatures. This latter pairing probably provides a better representation of the dynamics involved in the hydrocarbon chains, since the appearance of gauche rotamers is reflected primarily in the 1086–1090 cm^{-1} region. Fig. 1 displays both the definitions of the frequency intervals Δ cm^{-1} and the relative shifts involved for dipalmitoyl phosphatidylcholine multilayers at temperatures below, within, and above the gel-liquid crystalline transition.

Figs. 2 and 3 display plots of frequency differences for the 1129 and 1064 cm^{-1} transitions and the 1097 and 1064 cm^{-1} transitions, respectively, for dipalmitoyl phosphatidylcholine vesicles and multilayers. All four curves show rather abrupt changes in the 37–41 °C range, which identify the gel-liquid crystalline phase transitions. An obvious difference in the vesicle and multilayer curves is the broader nature of the vesicle plots. The vesicle transition appears to occur over a 1–2 °C wider range with the observed Δ cm^{-1} values encompassing a smaller overall change. Although the apparent difference in transition temperatures ($\sim$38 °C and 39 °C for vesicles and

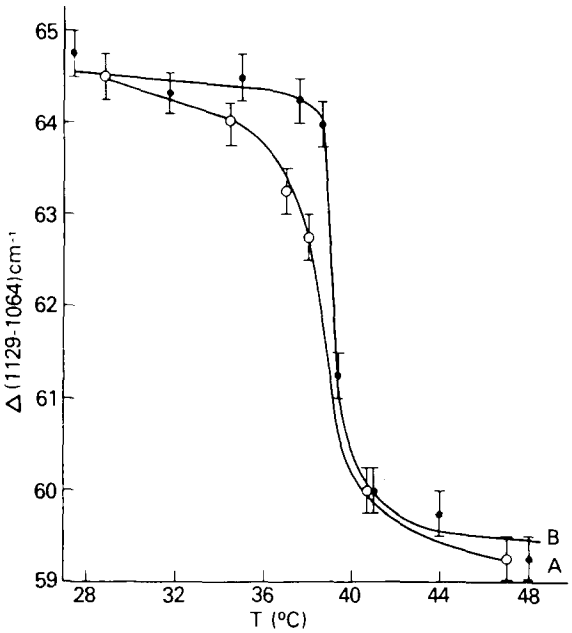

Fig. 2. Temperature profile for dipalmitoyl phosphatidylcholine/water vesicles (A) and multilayers (B) utilizing the frequency difference Δ cm^{-1} for the 1129 and 1064 cm^{-1} transitions.

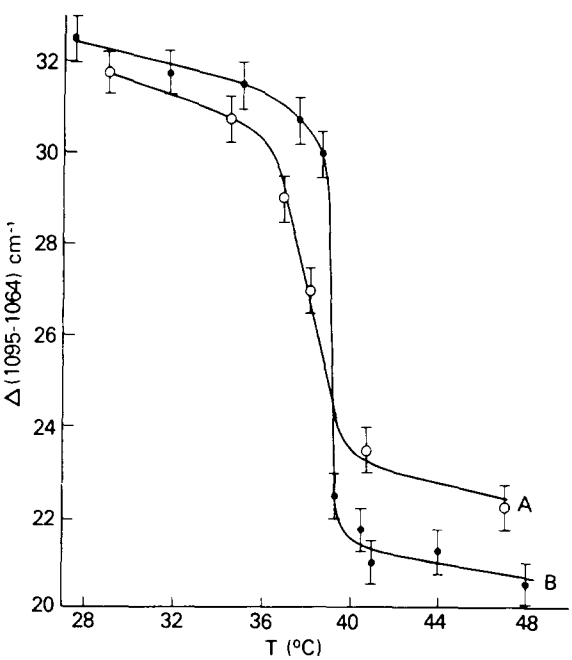

Fig. 3. Temperature profile for dipalmitoyl phosphatidylcholine/water vesicles (A) and multilayers (B) utilizing the frequency difference Δ for the 1097 and 1064 cm^{-1} transitions.

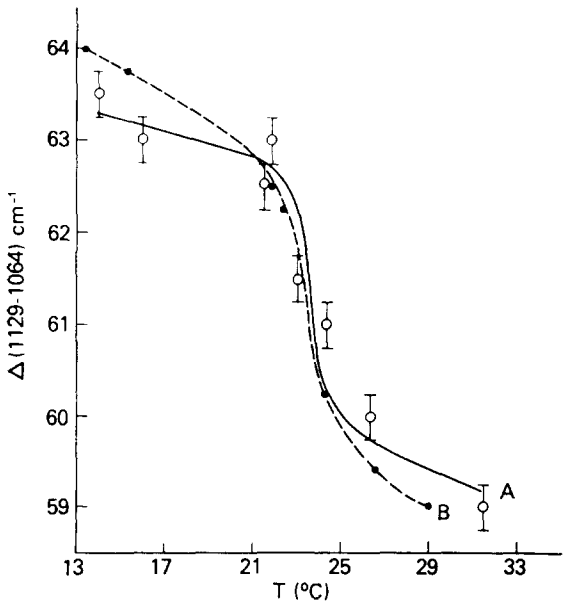

Fig. 4. Temperature profile for dimyristoyl phosphatidylcholine/water vesicles (—A) and multilayers (---B) utilizing the frequency difference Δ cm^{-1} for the 1129 and 1064 cm^{-1} transitions. Error bars are eliminated from the multilayer plot to preserve clarity.

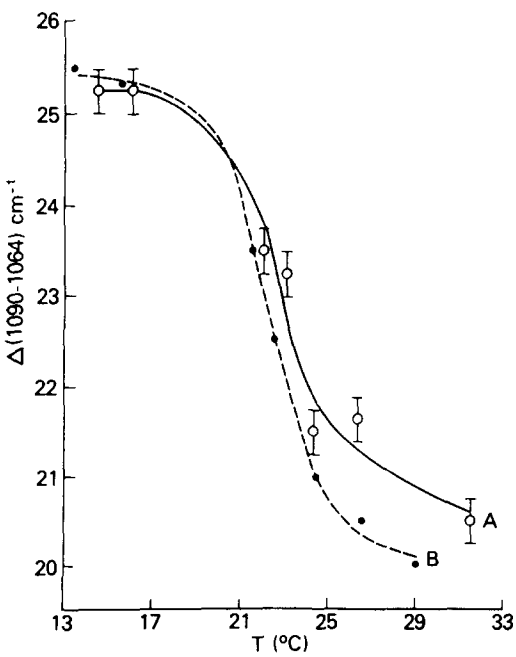

Fig. 5. Temperature profile for dimyristoyl phosphatidylcholine/water vesicles (—A) and multilayers (--B) utilizing the frequency difference Δ cm^{-1} for the 1090 and 1064 cm^{-1} transitions. Error bars are eliminated from the multilayer plot to preserve clarity.

multilayers, respectively) is about the interval of the experimental error, the relative broadness of the transition suggests a more disordered state for the hydrocarbon chains of the vesicles, a characteristic that would be associated with an irregular packing arrangement within a small diameter vesicle state.

Figs. 4 and 5 present $\Delta\,\mathrm{cm}^{-1}$ plots for dimyristoyl phosphatidylcholine multilayers and vesicles. All four curves exhibit fairly abrupt changes in the 21–25 °C temperature range. Although error bars are eliminated from the multilayer plots in order to preserve clarity, the temperature profiles for the two systems do not enable a clear distinction to be made between multilayer and vesicle assemblies with regard either to differences in transition temperatures or to chain disorder characteristics. We wish to note, however, that Raman spectral features in other regions of the spectrum indicate a more disordered state for both dimyristoyl and dipalmitoyl phosphatidylcholine vesicles compared to multilayer systems (Spiker, Jr., R. C. and Levin, I. W., unpublished data). The specific spectral details will be presented in a future publication.

Although the Raman frequency differences associated with the C-C stretching modes do not provide a definite difference in phase transition temperatures between the vesicle and multilayer forms, the transition temperatures determined by this technique are consistent with values obtained by other physical methods (for example refs. 21–26). The average values of 38 ± 1 °C and 39 ± 1 °C for dipalmitoyl phosphatidylcholine vesicles and multilayers, respectively, and a value of 23 ± 1 °C for both the multi- and unilamellar forms of dimyristoyl phosplatidylcholine are compared with other experimental measurements in Table I.

In general, other physical techniques give lower transition temperatures for

TABLE I

TRANSITION TEMPERATURES FOR PHOSPHOLIPID/WATER SYSTEMS AS DETERMINED BY VARIOUS EXPERIMENTAL TECHNIQUES

Compound	Temperature (°C)	Method
Dipalmitoyl phosphatidylcholine	39 ± 1	Raman frequency differences (multilayers)*
	38–39	Raman intensities [12]
	37–39	EPR [21]
	40–42	Calorimetric [22]
	39–41	Turbidimetric [23]
	43	Infrared intensities**
	~40	NMR (Vesicle diameter = 900 A) [27, 28]
	~38	NMR (Vesicle diameter = 300 A) [27, 28]
	41	Rate of Water evaporation [24]
	41	Relative density change [25]
	~44	Fluorescence (polyene fatty acid probes) [26]
Dimyristoyl phosphatidylcholine	23 ± 1	Raman frequency differences (multilayers)*
	24	Calorimetric [22]
	23	Turbidimetric [23]
	23	Rate of Water evaporation [24]
	~23	Fluorescence (polyene fatty acid probes) [26]

* This work. See text for discussion of transition temperature for vesicle systems.

** Ref. 14 (relative intensity change monitored for 1470 cm^{-1} CH_2 deformation).

vesicle systems in comparison to multilayer samples. For small diameter vesicles of dipalmitoyl phosphatidylcholine, transition temperatures determined by ^{1}H NMR [27, 28] and calorimetric [29] procedures are 2 and 5 °C, respectively, lower than the phase transition temperatures of multilayers. Dilatometric measurements [27] on dipalmitoyl phosphatidylcholine are consistent with these observations. Also, for dimyristoyl phosphatidylcholine an NMR study of ^{13}C-enriched lipids gives a lower transition temperature for small vesicles as compared to the multilayer system [30]. The issue, however, regarding differences in the properties of uni- and multilamellar systems may not yet be completely resolved. In particular, recent calorimetric studies [31] on dimyristoyl and dipalmitoyl phosphatidylcholine systems indicate no differences in transition temperatures between single-wall and multilayer membranes.

C. Temperature profile for dipalmitoyl phosphatidylcholine/cholesterol vesicles.

Calorimetric measurements [32] indicate that dipalmitoyl phosphatidylcholine/cholesterol/water systems exhibit a linearly decreasing phase transition enthalpy with increasing cholesterol concentrations to about 33 mol % of cholesterol, at which point the total enthalpy of the transition vanishes. Fig. 6 displays the temperature profile of the Raman frequency difference $\Delta(1095\text{–}1065)\ cm^{-1}$ for an excess water sonicate of 25 mol % cholesterol in dipalmitoyl phosphatidylcholine. Although cholesterol has Raman transitions in the 1065–1100 cm^{-1} region, the weak cholesterol signals representative of this mol fraction do not perturb the $\Delta\ cm^{-1}$ measurements for the hydrocarbon species. Fig. 6 significantly differs from the plots for the pure bilayer systems discussed above. For this system a broad transition occurs which spans about a 30 °C temperature range in contrast to the narrow 2–4 °C range for pure dipalmitoyl and dimyristoyl phosphatidylcholine multilayers and vesicles. An inflection point does occur at $\sim 50 \pm 5$ °C, although additional experimental points would be necessary to define this point more accurately. This broadening across the phase transition temperature has previously been ascribed to a second order, noncooperative process taking place in the mixture, unlike the cooperative processes

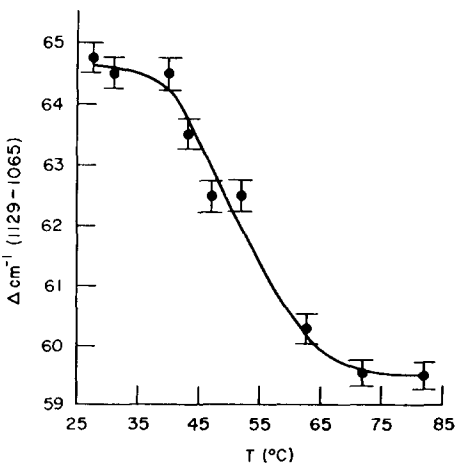

Fig. 6. Temperature profile for dipalmitoyl phosphatidylcholine/cholesterol (25 mol %)/water sonicate utilizing the frequency difference $\Delta\ cm^{-1}$ for the 1095 and 1065 cm^{-1} transitions.

observed for the other four systems [12, 33]. Specifically, a comparison between the $\Delta(1097–1065)\ cm^{-1}$ plot for the pure dipalmitoyl phosphatidylcholine/water vesicle system (Fig. 3A) and the $\Delta(1095–1065)\ cm^{-1}$ plot for the cholesterol containing vesicles (Fig. 6) shows that the cholesterol system exhibits more disorder, or is more fluid, for a given temperature below the transition temperature of about 38 °C, while for a specific temperature above the phase transition the cholesterol system is more ordered than the pure lipid bilayer. That is, a smaller $\Delta\ cm^{-1}$ value reflects, in the comparison, more chain disorder as a consequence of the greater contributions from the gauche structures to the transitions in the 1097 cm^{-1} spectral region. The $\Delta(1129–1065)\ cm^{-1}$ plots, which are not displayed for the two systems, have analogous interpretations. The conclusions drawn from the Raman frequency shift plots for the cholesterol-containing vesicles generally confirm the results from calorimetric [33] and Raman intensity [12] considerations.

A discrepancy, however, has yet to be resolved between the Raman intensity results [12] and the calorimetric investigation of Hinz and Sturtevant [32]. Thus, for the 50 mol % cholesterol concentrations used to demonstrate the broadening of the lipid phase transition in the Raman intensity measurements, the calorimetric study indicates a complete absence of the phase transition. The spectroscopic intensity measurements [12] yield an extended sigmoidal shape somewhat analogous to the shape of the $\Delta\ cm^{-1}$ plot in Fig. 6, which is indicative of a diminished cooperativity in the hydrocarbon chain melting, or disordering, process. Hinz and Sturtevant [32] suggest that the curve determined from Raman intensity measurements simply implies a continually increasing number of gauche conformations for increasing temperature, even though the system already exists in a fluid state. In support of their contention, temperature profiles for anhydrous dipalmitoyl phosphatidylcholine with and without cholesterol yield curves of a general characteristic shape analogous to that of Fig. 6 (Spiker, Jr., R. C. and Levin, I. W., unpublished data). These particular curves span temperature regions where no phase transitions occur. It appears that the Raman spectroscopic approach may be unable to distinguish between a system in which the phase transition is actually broadened and a system in which temperature induces further conformational changes.

ACKNOWLEDGMENT

One of us (R.C.S.) acknowledges the support provided by a National Institute of Arthritis, Metabolism and Digestive Diseases Postdoctoral Fellowship (5-F22 AM00103-02).

REFERENCES

1 Fox, C. F. (1975) Biochemistry Series One, Biochemistry of Cell Walls and Membranes (Fox, C. F., ed.), Vol. 2, pp. 279–306, Butterworths, London
2 Träuble, H. and Eibl, H. (1975) Functional Linkage in Biomolecular Systems (Schmitt, F. O. and Schneider, D. M., eds.), pp. 59–90, Raven Press, New York
3 Träuble, H. (1972) Biomembranes (Kreuzer, F. and Slegers, J. F. G., eds.), Vol. 3, pp. 197–227, Plenum Press, New York
4 Wunderlich, F., Ronai, A., Speth, V., Seelig, J. and Blume, A. (1975) Biochemistry 14, 3730–3735
5 Shimshick, E. and McConnell, H. M. (1973) Biochemistry 12, 2351–2360

6 Linden, C. D., Wright, K. L., McConnell, H. M. and Fox, C. F. (1973) Proc. Natl. Acad. Sci. U.S. 70, 2271–2275
7 Podo, F. and Blasie, J. K. (1975) Biochemistry Series One, Biochemistry of Cell Walls and Membranes (Fox, C. F., ed.), Vol. 2, pp. 97–121
8 Brown, G. K., Peticolas, W. L. and Brown, E. (1973) Biochem. Biophys. Res. Commun. 54, 358–364
9 Larsson, K. and Rand, R. P. (1973) Biochim. Biophys. Acta 326, 245–255
10 Larsson, K. (1973) Chem. Phys. Lipids 10, 165–176
11 Lippert, J. L. and Peticolas, W. L. (1972) Biochim. Biophys. Acta 282, 8–17
12 Lippert, J. L. and Peticolas, W. L. (1971) Proc. Natl. Acad. Sci. U.S. 68, 1572–1576
13 Mendelsohn, R. (1972) Biochim. Biophys. Acta 290, 15–21
14 Bulkin, B. J. and Krishnamachari, N. (1972) J. Am. Chem. Soc. 94, 1109–1112
15 Spiker, Jr., R. C. and Levin, I. W. (1975) Biochim. Biophys. Acta 388, 361–373
16 Prestegard, J. H. and Fellmeth, B. (1974) Biochemistry 13, 1122–1126
17 Lau, A. L. Y. and Chan, S. S. (1974) Biochemistry 13, 4942–4948
18 Levin, I. W. (1969) Spectrochim. Acta 25A, 1157–1160
19 Snyder, R. G. (1967) J. Chem. Phys. 47, 1316–1360
20 Wilson, Jr., E. B., Decius, J. C. and Cross, P. C. (1955) Molecular Vibrations, McGraw-Hill Book Company, New York
21 Hubbell, W. L. and McConnell, H. M. (1971) J. Am. Chem. Soc. 93, 314–326
22 Hinz, H. J. and Sturtevant, J. M. (1972) J. Biol. Chem. 247, 6071–6075
23 Abramson, M. B. (1971) Biochim. Biophys. Acta 225, 167–170
24 Fiedler, O. (1974) Biochem. Biophys. Acta 345, 321–325
25 Nagle, J. F. (1973) Proc. Natl. Acad. Sci. U.S. 70, 3443–3444
26 Sklar, L. A., Hudson, B. S. and Simoni, R. D. (1975) Proc. Natl. Acad. Sci. U.S. 72, 1649–1653
27 Sheetz, M. P. and Chan, S. S. (1972) Biochemistry 11, 4572–4581
28 Chan, S. S., Sheetz, M. P., Seiter, C. H. A., Feigenson, G. W., Hsu, M., Lau, A. and Yau, A. (1973) Ann. N. Y. Acad. Sci. 222, 499–522
29 Sturtevant, J. M. (1974) Ann. Rev. Biophys. Bioeng. 3, 35–51
30 Metcalf, J. C. (1975) Functional Linkage in Biomolecular Systems (Schmitt, F. O. and Schneider, D. M., eds.), pp. 90–98, Raven Press, New York
31 De Kruiff, B., Cullis, P. R. and Radda, G. K. (1975) Biochem. Biophys. Acta 406, 6–20
32 Hinz, H.-J. and Sturtevant, J. M. (1972) J. Biol. Chem. 247, 3697–3700
33 Ladbrooke, B. D., Williams, R. M. and Chapman, D. (1968) Biochim. Biophys. Acta 150, 333–340